



Catalytic wet peroxide oxidation of phenol over Fe/AC catalysts: Influence of iron precursor and activated carbon surface

A. Rey ^a, M. Faraldo ^a, J.A. Casas ^b, J.A. Zazo ^b, A. Bahamonde ^{a,*}, J.J. Rodríguez ^b

^a Instituto de Catálisis y Petroquímica, CSIC, C/ Marie Curie No. 2, 28049 Madrid, Spain

^b Área de Ingeniería Química, Facultad de Ciencias, Universidad Autónoma de Madrid, Campus de Cantoblanco, 28049 Madrid, Spain

ARTICLE INFO

Article history:

Received 25 April 2008

Received in revised form 16 July 2008

Accepted 24 July 2008

Available online 5 August 2008

Keywords:

Oxidation

Hydrogen peroxide

Catalyst

Activated carbon

Iron

Phenol

ABSTRACT

Different activated carbon-supported Fe catalysts have been prepared and tested in CWPO of phenol. Three well characterized activated carbons and two iron precursors (iron nitrate and iron pentacarbonyl) have been used. The behavior of these catalysts in CWPO has been related with their porous structure, surface composition, in terms of oxygen groups and Fe distribution onto the catalyst particles. The catalysts with a more uniform distribution of Fe showed a higher oxidation activity than the ones with an internal (egg-yolk type) or external (egg-shell type) distribution. These last provoke a faster decomposition of H_2O_2 mainly to O_2 , non-reactive at the mild reaction temperature used (50 °C). No significant differences were observed from the iron precursors. Complete conversion of phenol and almost 80% mineralization were obtained in less than 2 h with the best catalyst. The residual by-products consisted in short-chain organic acids without significance in terms of toxicity. Fe leaching was observed in all the cases which can be mainly attributed to the presence of oxalic acid as oxidation by-product, refractory to the CWPO process investigated. The intensity of Fe leaching was related with the concentration of oxalic acid.

© 2008 Published by Elsevier B.V.

1. Introduction

The industry generates a variety of wastewaters requiring the application of cost-effective treatments. A number of techniques such as chemical, physical, biological, incineration, etc. [1], and their combinations are available, but each process has its inherent limitations in applicability, effectiveness, and cost [2]. Many industrial effluents are not suitable for biological processes due to the presence of some pollutants highly refractory and toxic. On the other hand, their treatments by conventional chemical processes may have several drawbacks in terms of efficiency and/or cost [3].

Therefore more efficient and economic solutions for end-stream treatment, avoiding high-energy input technologies are becoming imperative [4] and essential to produce environmentally friendly effluents and reusable process water. Catalytic processes are gaining increasing interest as potential solutions in the field of wastewaters treatment. The use of appropriate catalysts can substantially decrease the energy consumption of various well-known oxidation processes, such as wet air and wet peroxide oxidation of refractory

organic compounds [5,6]. In the last decade great research efforts have been addressed to this aim pointing out the prominent role of advanced oxidation processes (AOPs) [7] which usually operate at or near ambient temperature and pressure [8,9]. They are characterized by the capability of exploiting the high reactivity of hydroxyl radicals in driving oxidation processes to the nearly complete abatement or mineralization of even highly resistant pollutants.

The hydroxyl radical is an extraordinarily reactive species capable of attacking organic molecules with rate constants usually in the order of 10^6 to $10^9 \text{ M}^{-1} \text{ s}^{-1}$ [10]. However, some important aspects should be considered before selecting the most suitable AOP. As these processes use expensive reactants like H_2O_2 and/or O_3 , they are usually restricted to wastes with relatively small COD contents ($\leq 5.0 \text{ g L}^{-1}$) since higher organic loads would require the consumption of too large amounts of reactants and thus, wet oxidation or incineration become more feasible solutions [11].

Stable supported catalysts with very high activity for the oxidation of organic pollutants have been prepared and successfully tested in the catalytic oxidation of phenol [12,13], given that this pollutant is a good model compound for many industrial wastewaters. Recently, activated carbon (AC) has proved to be an excellent catalytic support in the oxidation of aromatic compounds [14–16], and considerable advance in the understanding of the

* Corresponding author. Tel.: +34 915855475; fax: +34 91 585 4760.

E-mail address: abahamonde@icp.csic.es (A. Bahamonde).

relationship between the physical and chemical properties of carbon materials and the catalysts efficiency have been carried out in the last few years [17,18].

It is known that the carbon structures offer an unparalleled flexibility for tailoring catalysts properties to specific needs. Among their excellent properties can be emphasized their high surface area, well developed and different porous structure and variable surface composition which determine important differences in their reactivity allowing to study the effects of these features on the catalytic behavior. Specifically in environmental applications related to wastewater treatments, the structure of activated carbon plays an important role because the adsorption capacity is determined by both the porous structure and the chemical nature of the surface [19–23]. So, it is very important to understand the role of the activated carbon surface in the preparation of optimized catalysts in terms of activity and stability.

It is well known that some transition metallic elements like iron promote hydrogen peroxide decomposition to hydroxyl radicals capable to efficiently oxidize organic matter [24,25]. In this sense, some studies in the literature have been focussed on the application of activated carbon supported catalysts in wet peroxide oxidation of organic pollutants (CWPO) [25–28], most of them based on phenol oxidation.

Thus in this work, three fairly different activated carbons in terms of porous structure and surface composition have been chosen as catalytic supports. In relation to the iron precursor, quite different compounds, such as iron nitrate and iron pentacarbonyl dissolved in aqueous solution and organic medium respectively, have been also studied to develop good and stable Fe/AC catalyst in the CWPO of phenol. Taking into account the hydrophobic general character of activated carbon and the different amount and nature of surface oxygen groups of the supports, which can modify the AC hydrophobic character, the selection of aqueous medium and organic medium for the preparation of the iron supported catalysts can lead to get Fe/AC catalysts with different properties. Besides, the oxidation state of Fe in the precursors (Fe³⁺ in iron nitrate and Fe⁰ in iron pentacarbonyl) may lead to some important differences as well in the behavior of phenol oxidation process studied here. Thus, it can be expected different interactions of iron precursor with AC surface due to the different nature of AC supports and iron precursors.

Therefore, the aim of this work was testing two series of home-made iron-activated carbon catalysts for the CWPO of phenol at mild conditions such as atmospheric pressure and 50 °C of temperature. The influence of iron precursor as well as the structure and surface composition of the activated carbon supports were analyzed in relation with the activity and stability of the resulting catalysts.

2. Experimental

2.1. Catalysts preparation

Two series of activated carbon-supported Fe catalysts (Fe/AC) were prepared by incipient impregnation at room temperature from an aqueous solution of iron nitrate (Series 1) and a solution of iron pentacarbonyl in n-hexane (Series 2). Three different commercial activated carbons, supplied by Merck (Cod. 102514; d_p : 1.5 mm), Norit (Norit Row 0.8 Supra; d_p < 0.6 mm), and Chemviron (Centaur HSL; d_p : 0.8–1 mm), CM, CN and CC, respectively, were used as supports to obtain catalysts with the same nominal iron content (4%, w/w). All the samples were left overnight at room temperature, dried during 12 h at 70 °C, and finally heat-treated at 200 °C in air atmosphere for 4 h. Table 1 summarizes the identification of the catalysts prepared. Although

Table 1
Identification of the catalysts prepared

Catalyst	Support	Iron precursor	Fe _{measured} (% w/w, d.b.)
Series 1	FeCM-1	CM	Nitrate
	FeCN-1	CN	Nitrate
	FeCC-1	CC	Nitrate
Series 2	FeCM-2	CM	Pentacarbonyl
	FeCN-2	CN	Pentacarbonyl
	FeCC-2	CC	Pentacarbonyl

the Fe to carbon weight ratio used in the impregnation step was always the same, lower percentages of Fe on the final catalysts were repeatedly obtained for the Series 2.

2.2. Characterization

Elemental analysis of the catalysts were obtained in a LECO CHNS-932 Elemental Analyzer. Ashes contents were determined by thermal gravimetry with a Mettler Toledo TGA/STD A 851^e in air flow of 200 cm³ min⁻¹ at a heating rate of 5 °C min⁻¹ from room temperature to 1000 °C. Total iron content was analyzed by inductively coupled plasma (OES-ICP) with a PerkinElmer Optima 3300 DV model.

The porous structure of the catalysts was characterized from nitrogen adsorption–desorption isotherms at –196 °C using a Micromeritics Tristar apparatus on samples previously outgassed overnight at 250 °C to a residual pressure of <10^{–4} Pa. From the N₂ isotherms the values of BET surface area were obtained. The micropore volume and the external or nonmicroporous surface were obtained using the t-method. Mercury intrusion porosimetry (MIP) was used to determine the meso and macropore volumes using CE Instruments Pascal 140/240 apparatus. The mesopore volume in the range not covered by mercury porosimetry was obtained from the N₂ isotherm.

Determination of pH of aqueous slurries of the catalysts was carried out placing 0.5 g of Fe/AC catalyst in 10 mL of CO₂-free distilled water kept in a bottle at room temperature and continuously stirred until pH of the slurry was stabilized. It was measured by a CRISON pH-meter apparatus after filtration.

The nature, distribution and amount of surface oxygen groups were analyzed by temperature programmed desorption under N₂ flow (TPD-N₂) and by X-ray photoelectron spectroscopy (XPS). This second was also used to recognize Fe species. For the TPD analyzes a sample of 0.1 g was placed in a vertical quartz tube in nitrogen flow of 1 NL min⁻¹ at a heating rate of 10 °C min⁻¹ from room temperature to 900 °C. The evolved amounts of CO and CO₂ were continuously analyzed by a Siemens Ultramat 23 NDIR analyzer. X-ray photoelectron spectra (XPS) were obtained with a VG Escalab 200R spectrometer equipped with a hemispherical electron analyzer (pass energy of 20 eV) and a Mg K α ($h\nu$ = 1254.6 eV) X-ray source, powered at 120 W. Binding energies were calibrated relative to the C 1s peak from carbon samples at 284.6 eV. For the analysis of the peaks a Shirley type background was used. Peaks were adjusted to a combination of Gaussian and Lorentzian functions using the XPSPeak 4.1 software.

2.3. Adsorption, catalytic activity and stability experiments

All runs were carried out in batch using 100 mL glass bottles shaken in a thermostatic bath at the following operating conditions: 200 rpm, 50 °C, atmospheric pressure, 50 mL of reaction volume and an initial pH of 3 adjusted by using a concentrated HCl solution.

Table 2

Elemental analysis of Fe/AC catalysts (% w/w, d.b.)

Catalyst	C	H	N	S	O ^a	Ashes
FeCM-1	75.40	1.27	0.77	0.64	12.64	9.28
FeCN-1	70.50	1.71	1.18	0.63	14.66	11.32
FeCC-1	70.00	1.92	1.50	0.70	16.43	9.45
FeCM-2	83.80	1.17	0.51	0.65	6.69	7.18
FeCN-2	81.40	1.50	0.48	0.69	6.47	9.46
FeCC-2	79.20	1.90	1.12	0.69	9.08	8.01

^a By difference.

Starting concentrations were the following: 100 mg L⁻¹ of phenol, 500 mg L⁻¹ of hydrogen peroxide (corresponding to the theoretical stoichiometric amount of H₂O₂ for complete oxidation of phenol up to CO₂ and H₂O) and 500 mg L⁻¹ of powdered iron-activated carbon catalysts ($d_p < 100 \mu\text{m}$). Phenol adsorption runs were performed in the same conditions without H₂O₂ addition and, in the same form, H₂O₂ decomposition experiments were carried out without phenol in the aqueous solution. Iron leaching tests were carried out at the same aforementioned conditions using 25 mg L⁻¹ of oxalic acid and 500 mg L⁻¹ of powdered iron-activated carbon catalysts. Besides, to analyze the effect of initial concentration of phenol two experiments were carried out with the following starting concentrations: 1000 mg L⁻¹ of phenol, 5000 mg L⁻¹ of H₂O₂ (stoichiometric amount) and 5000–1000 mg L⁻¹ of FeCM-1 powdered iron-activated carbon catalysts.

Phenol and aromatic oxidation intermediates were followed by means of HPLC (Varian Pro-Star 335 Diode array detector) with a Nucleosil C-18 column (5 μm , 150 mm long, 4.6 mm diameter) at 40 °C as stationary phase and 0.8 mL min⁻¹ of 20:80 methanol:acidic water (0.1% acetic acid) as mobile phase. Short-chain organic acids were analyzed by an Ion Chromatograph with chemical suppression (Metrohm 790 IC) and a conductivity detector using a Metrosep A supp 5–250 column (250 mm long, 4 mm diameter) as stationary phase and 3.2 mM Na₂CO₃ and 1 mM NaHCO₃ as mobile phase. Total organic carbon (TOC) was measured using a TOC analyzer with infrared detector TOC-Vsch, Shimadzu. Hydrogen peroxide concentration was determined by a colorimetric titration method [29] based on the formation of a yellow colored complex Ti(IV)–H₂O₂, using a UV 2100 Shimadzu UV/Vis spectrophotometer at 410 nm. Fe leached to the reaction media was determined by means of o-phenanthroline method [30] using an UV/Vis spectrophotometer at 510 nm.

Table 3

Porous structure of Fe/AC catalysts

Catalyst	S_{BET} (m ² g ⁻¹)	A_{ext} (m ² g ⁻¹)	V_{total} (cm ³ g ⁻¹)	$V_{\text{micropore}}$ (cm ³ g ⁻¹)
FeCM-1	934	85	0.613	0.366
FeCN-1	883	83	0.640	0.345
FeCC-1	837	5	0.388	0.346
FeCM-2	948	88	0.614	0.371
FeCN-2	951	137	0.805	0.354
FeCC-2	850	8	0.369	0.352

3. Results and discussion

3.1. Catalysts characterization

Elemental composition of Fe/AC catalysts together with their ashes contents are reported in Table 2. The oxygen percentages of the catalysts were always higher than those of the corresponding carbon supports [31], as a consequence of the final heat-treatment in air atmosphere. This is more noticeable in the case of Series 1 where iron nitrate was used as Fe precursor. The ash contents of the Series 1 are in all the cases higher than those of the corresponding catalysts of Series 2 as the result of the somewhat higher amounts of Fe incorporated (Table 1).

Table 3 summarizes the porous structure of the catalysts. In general a decrease of surface area and total pore volume was observed with respect to the original activated carbon supports, most probably as a consequence of some extent of pore blockage after deposition of iron species on the mouth of small pores [31]. Nevertheless, this effect was of low significance and like the activated carbon supports, the catalysts presented fairly high surface areas, around 900 m² g⁻¹, and predominantly type I adsorption isotherms characteristic of microporous materials. However, the Fe/CM and Fe/CN catalysts, like their corresponding AC supports [31], showed H4 hysteresis loops indicative of some significant contribution of mesoporosity to their final porous structure (Fig. 1 and Table 3).

TPD-N₂ and XPS studies in addition to the measurement of pH_{slurry} were carried out to learn about the surface chemical composition of Fe/AC catalysts. In Table 4 are summarized the pH_{slurry} values and the amounts of CO and CO₂ evolved upon TPD-N₂. An important decrease of pH_{slurry} accompanied to Fe introduction in all the cases, especially in the catalysts prepared

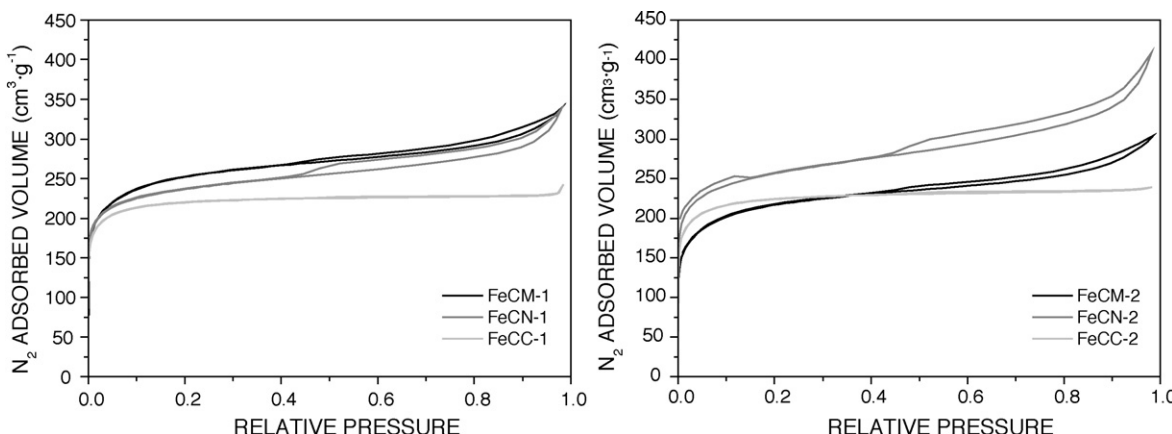
**Fig. 1.** Nitrogen adsorption–desorption isotherms for all the studied Fe/AC catalysts.

Table 4 $\text{pH}_{\text{slurry}}$ and CO and CO_2 evolved upon TPD ($\mu\text{mol g}^{-1}$)

Catalyst	$\text{pH}_{\text{slurry}}$	CO_2	CO
FeCM-1	3.74	1252	1871
FeCN-1	6.05	1259	2732
FeCC-1	3.21	1486	2311
FeCM-2	5.85	220	850
FeCN-2	8.85	345	1589
FeCC-2	5.41	477	2146

from iron nitrate due to the acidic and oxidizing character of this agent. The frankly basic CN support led to higher $\text{pH}_{\text{slurry}}$ values in the corresponding Fe/CN catalysts, especially in that from Series 2, the only one maintaining an overall basic character.

As can be seen the catalysts of Series 1 show substantially higher content of surface oxygen groups, as expected from the higher oxidizing power of iron nitrate. This is more pronounced with regard to the CO_2 -evolving groups in agreement with the more acidic character of their surfaces. Nevertheless, it must be considered that the evolved CO and CO_2 may come in some extent from reaction of iron oxides with carbon. In fact, the CO-TPD of the catalysts showed in all the cases a pronounced band starting around 600 °C and extending up to the final temperature (900 °C) which can be partly due to the aforementioned reaction.

XPS analysis confirmed the higher concentration of oxygen groups in the surface of the catalysts from Series 1 as can be seen in Table 5. This table also reports the Fe/C atomic ratios. The XPS spectra of the Fe 2p spectral region are shown in Fig. 2. In all the cases it can be observed the presence of a main band centered at

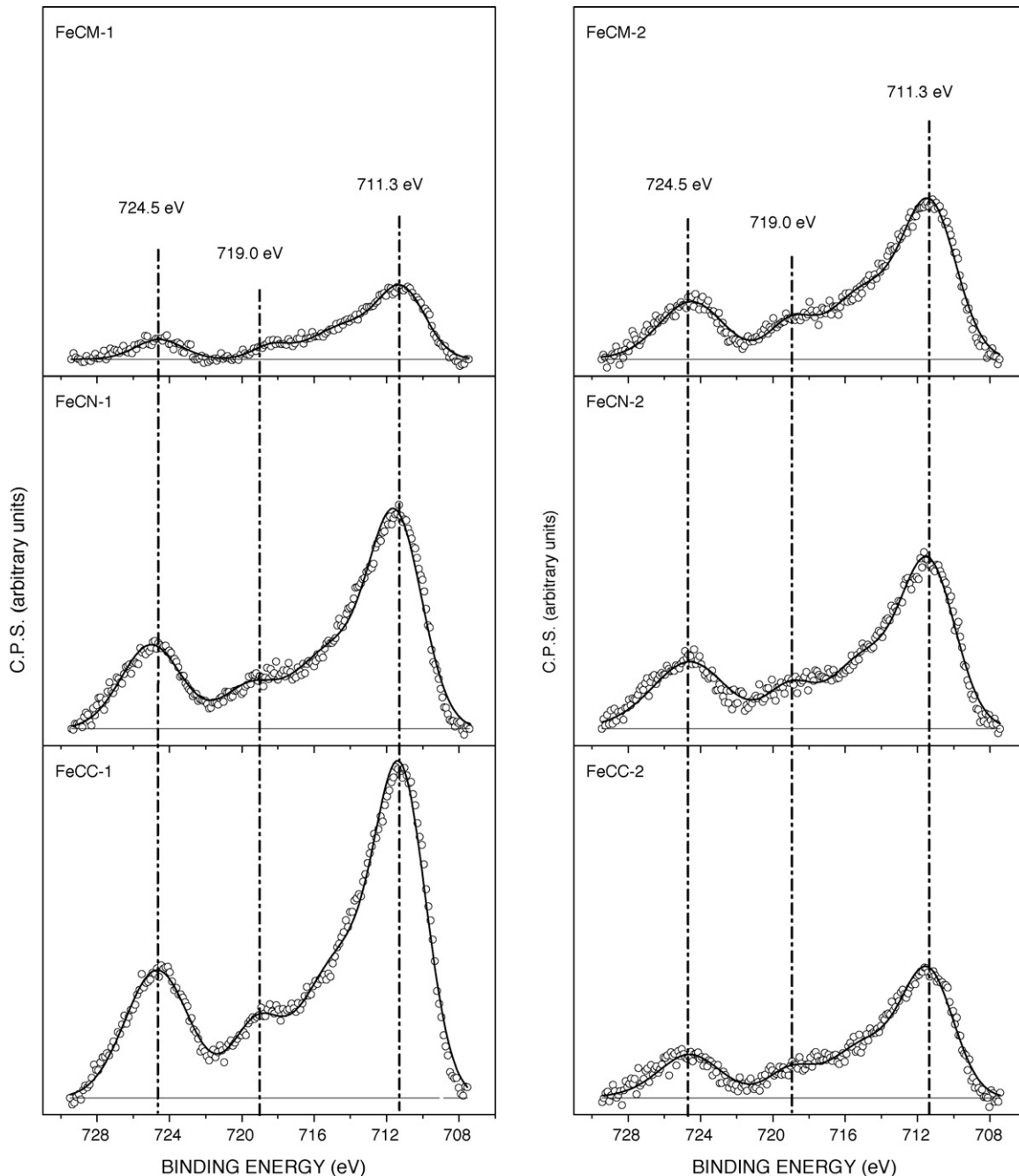
**Fig. 2.** XPS spectra of Fe 2p spectral region of the catalysts.

Table 5

O/C and Fe/C atomic ratios of the catalysts

Catalyst	(O/C) _{bulk}	(O/C) _{XPS}	(Fe/C) _{bulk}	(Fe/C) _{XPS}	(O/Fe) _{XPS}
FeCM-1	0.126	0.081	0.013	0.005	16.2
FeCN-1	0.156	0.182	0.012	0.026	7.0
FeCC-1	0.176	0.199	0.013	0.045	4.4
FeCM-2	0.060	0.070	0.009	0.013	5.4
FeCN-2	0.060	0.079	0.010	0.013	6.1
FeCC-2	0.086	0.092	0.009	0.012	7.6

711.3 eV accompanied by a secondary one displaced 13.2 eV to higher binding energy (724.5 eV), with an area ratio of 1:0.5, which correspond to the characteristic values of Fe^{3+} , in addition to a satellite peak around 719.0 eV confirming the presence of Fe^{3+} species in the surface of all the catalysts [32].

When comparing the Fe/C atomic ratios obtained from elemental and XPS analysis it is observed that whereas fairly close values were obtained for all the catalysts of Series 2 (iron pentacarbonyl precursor), significant differences appear in the case of Series 1 (iron nitrate precursor). The catalyst prepared from the CC support in Series 1 shows a XPS Fe/C ratio more than three times higher than its bulk Fe/C ratio, suggesting that Fe must be predominately located in the most external surface of the catalyst particles, approaching to an egg-shell type distribution. This type of distribution can be also postulated for the FeCN-1 catalyst although less pronounced. On the opposite, in the FeCM-1 catalyst iron seems to be more concentrated in the inner region of the microporous structure, approaching more to an egg-yolk type distribution.

The trends observed for the Fe/C ratios are consistent with those of the O/C ratios although for these last the differences found between the bulk and XPS values are much lower, suggesting a more uniform distribution of the oxygen groups. These results do not allow to unambiguously postulating a simple model of Fe location on the oxygen surface groups. In Series 2 both the oxygen groups and Fe seem to be quite uniformly distributed on the catalyst particles and in this case the hypothesis of Fe being mainly located on the oxygen groups could be in principle more likely. In this second series the O/Fe atomic ratio obtained from XPS varies within a narrow range (5.4–7.6) whereas in Series 1 the range is significantly wider (4.4–16.2).

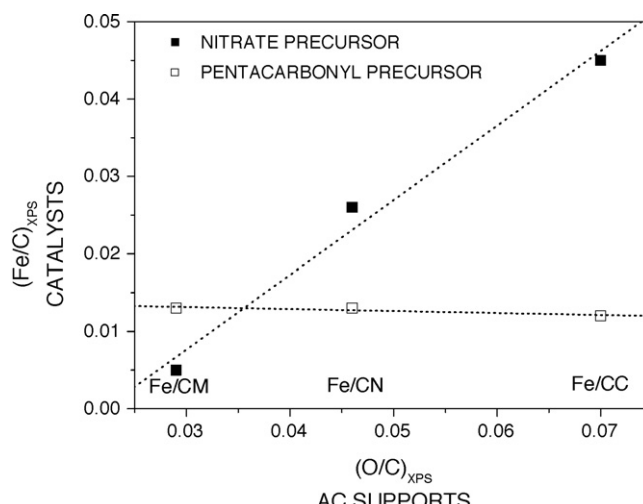


Fig. 3. Relationship between the Fe surface concentration of the catalysts and the O surface concentration of the AC supports.

Nevertheless it has to be considered that an important amount of the oxygen surface groups are created during the catalyst preparation in the calcination step that follows to Fe impregnation. Thus the association of iron to the oxygen groups should be analyzed comparing the Fe/C atomic ratio of the catalysts with the O/C ratio of the corresponding activated carbon supports. Fig. 3 shows that relationship. As can be seen, whereas in the catalysts of Series 1 the Fe concentration on the external surface of the catalysts (Fe/C ratio from XPS) increases when increasing the surface oxygen concentration of the support that is not the case for Series 2. This could be the result of electrostatic interactions between negatively charged oxygen groups and Fe^{3+} hydroxocomplex in the impregnation step when $\text{Fe}(\text{NO}_3)_3$ is used whereas with iron pentacarbonyl Fe is predominantly as Fe^0 . After the heat treatment in air atmosphere Fe is mostly as trivalent iron as previously discussed from the XPS spectra of the catalysts (Fig. 2).

3.2. Catalytic activity

3.2.1. Phenol adsorption

Prior to phenol oxidation runs, phenol adsorption tests were carried out in order of discriminating adsorption from reaction. The results obtained are given in Table 6 as adsorbed TOC (%) after 4 h contact time. A decrease around 10–15% of adsorption capacities was found in all the catalysts as compared with the corresponding carbon supports [31]. The lowest phenol adsorption corresponds in both series to the CC catalyst which has the lowest BET surface area together with a much lower contribution of mesoporosity that can determine more pronounced diffusional restrictions. Also, in general a lower $\text{pH}_{\text{slurry}}$ is associated with a lower phenol adsorption as can be seen from the values of Tables 4 and 6, according with some works in the literature which concluded that phenol adsorption is diminished due to the presence of acid-type surface oxygen groups in the AC surface [33–35].

3.2.2. H_2O_2 decomposition

It is well known that activated carbons promote the decomposition of hydrogen peroxide [36]. This reaction can be catalyzed by two types of active sites in Fe/AC catalysts. The AC support has unsaturated valences and electron-rich sites, or basic sites, in its structure [37]. The amount and nature of surface oxygen groups can also affect the rate of H_2O_2 decomposition. On the other hand, iron active sites promote the formation of highly oxidant $\cdot\text{OH}$ radicals from H_2O_2 . Thus, some significant differences can be expected between the Fe/AC catalysts and the corresponding carbon supports regarding to H_2O_2 decomposition.

Table 6 reports the values of the first-order rate constant for hydrogen peroxide decomposition with the catalysts tested. As can be seen, the catalysts prepared from iron nitrate decompose H_2O_2 faster than the corresponding from iron pentacarbonyl and the CC-supported catalysts decompose H_2O_2 at about double rate than the two other in both series. Nevertheless, the rate of H_2O_2 decomposition with this catalyst is lower than the observed for the

Table 6
Phenol adsorption and H_2O_2 decomposition with the catalysts

Catalyst	Phenol adsorption		H_2O_2 decomposition	
	% Adsorbed TOC ($t = 240$ min)	k (min^{-1})	k (min^{-1})	r^2
FeCM-1	37.3		0.089	0.995
FeCN-1	42.7		0.080	0.994
FeCC-1	33.0		0.154	0.990
FeCM-2	42.5		0.056	0.991
FeCN-2	46.7		0.064	0.998
FeCC-2	35.7		0.120	0.996

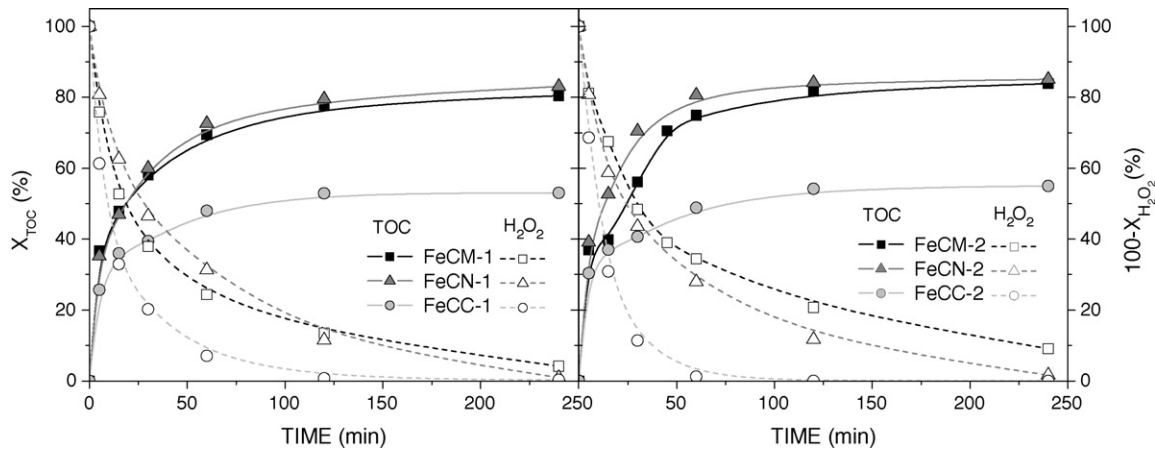


Fig. 4. Evolution of TOC and H_2O_2 in CWPO of phenol with Fe/AC catalysts.

activated carbon support [31]. The opposite was found in the case of the CM catalysts whereas the CN ones gave values of the rate constant comparable to that of the activated carbon itself. A simple explanation cannot be provided since two opposite effects are involved. The inclusion of Fe enhances the decomposition of H_2O_2 into $\cdot\text{OH}$ radicals but also gives rise to the formation of new oxygen groups on the carbon surface (in the calcination step). It has been observed that increasing these groups diminishes the rate of H_2O_2 decomposition [38].

3.2.3. Phenol oxidation

Fig. 4 shows the evolution of TOC and H_2O_2 in the oxidation runs performed with the catalysts investigated. As observed, the CC-supported catalysts of both series promote a much faster decomposition of H_2O_2 but accompanied by the poorest results on TOC removal, only somewhat higher than the attained by adsorption. This indicates a fairly inefficient decomposition of hydrogen peroxide which could be explained by two causes: (a) a high contribution of decomposition towards O_2 non-reactive at the mild operating temperature of the experiments (50°C) and/or (b) a very fast decomposition of H_2O_2 provokes a high concentration of $\cdot\text{OH}$ radicals in the initial stage which favors auto-scavenging reactions. On the opposite, the other two catalysts show a substantially more efficient use of H_2O_2 whose decomposition must be occurring mainly through the formation of $\cdot\text{OH}$ radicals at a lower rate, so that they are more readily available throughout the reaction time. Important mineralization percentages are achieved after about 1 h of reaction which continues increasing throughout the whole reaction time as H_2O_2 is still decomposing. No significant differences were observed from the two iron precursors (nitrate or pentacarbonyl).

The efficiency on the use of H_2O_2 can be more clearly seen in Fig. 5 where phenol and H_2O_2 conversions are plotted together. Values below the diagonal are indicative of a fairly poor behavior as is the case of the CC-supported catalysts, which at similar H_2O_2 conversion values gave always fairly lower phenol conversions. This supports the conclusion that the CC catalysts are promoting the decomposition of H_2O_2 mainly towards non-reactive O_2 . Complete removal of phenol is achieved with the other catalysts although some amounts of oxidation products still remain after the 4 h maximum reaction time as reveal the TOC curves of Fig. 4. These products correspond to short-chain organic acids, mainly oxalic and formic, without significance in terms of toxicity. This can be seen in Fig. 6 where the evolution of the oxidation intermediates is presented. As the most important conclusion, the concentrations of hydroquinone and *p*-benzoquinone become

negligible after about 2 h, except in the case of the FeCM-1 catalyst. These compounds are by far the most toxic species in the oxidation route of phenol. Among the organic acids, oxalic deserves a particular attention because it has been reported as the main responsible of iron leaching from Fe-based catalysts [9,25,39] and it shows refractory to oxidation by the CWPO process investigated, as can be seen in Fig. 6. As observed, the catalysts prepared from the CN carbon led to the highest concentration of oxalic acid.

Iron loss should lead to a decrease of activity. Nevertheless, the results of Fig. 6 show that except for the FeCM-1 catalyst the residual concentrations of toxic aromatic intermediates are negligible after 2 h reaction time and at that time oxalic acid remains still at a relatively low concentration so that a high Fe leaching should not be expected.

The possible homogeneous contribution to phenol oxidation with this type of Fe/AC catalysts seems to be negligible since studies carried out in a previous paper [25], led to establish that even when using a quantity of dissolved Fe equal to the total weight of this metal in the catalyst (20 mg L^{-1}), the TOC reduction obtained through homogeneous phase oxidation was around one-half that reached in the heterogeneous process with this type of iron-supported AC-based catalysts. Therefore, taking into account that never the maximum iron concentration detected in solution (8 mg L^{-1} with FeCN-1) was higher to half part of total weight of iron in the catalysts and that when the concentration of Fe in the reaction medium began to be significant, H_2O_2 was almost totally

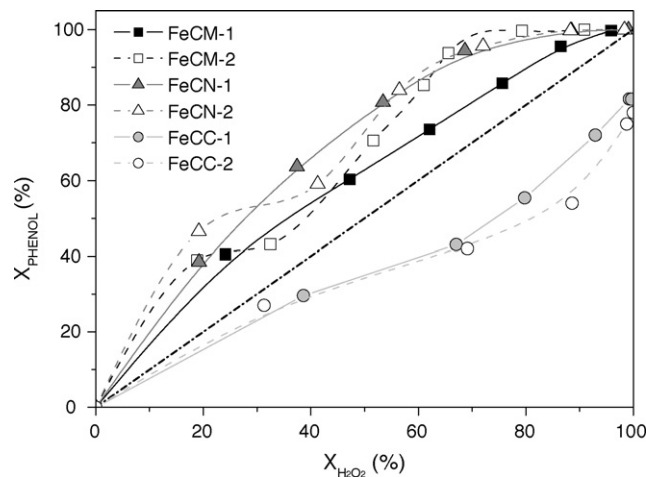


Fig. 5. Evolution of phenol vs. H_2O_2 conversion.

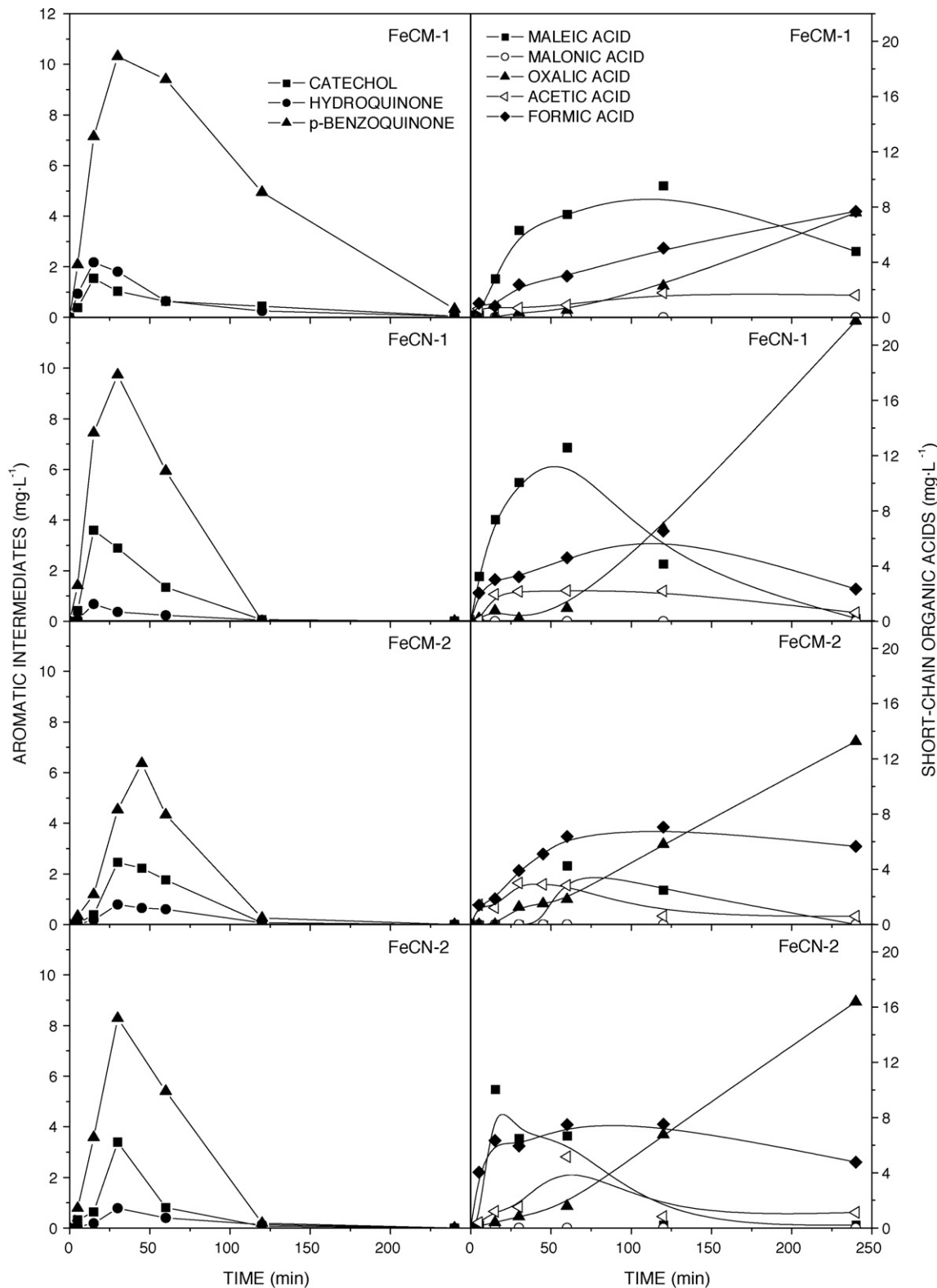


Fig. 6. Evolution of aromatic intermediates and organic acids from CWPO of phenol.

decomposed, the possible homogeneous contribution to oxidation process can be considered negligible in all cases.

To analyze the effect of initial concentration of phenol, two experiments with 1000 mg L^{-1} of phenol have been carried out using the stoichiometric amount of H_2O_2 for complete oxidation

testing two catalyst concentrations 5000 and 1000 mg L^{-1} . These results for FeCM-1 catalyst are summarized in Table 7 where TOC corresponding to refractory short chain organic acids detected at 240 min (oxalic, acetic and formic acids) join to Fe lixiviates to the reaction medium, in mg L^{-1} and percentage respect to the

Table 7

Activity results of FeCM-1 catalyst for the three studied operating conditions

Operating conditions	$[\text{Phenol}]_0/[\text{H}_2\text{O}_2]_0$	Catalyst (mg L ⁻¹)	$X_{\text{TOC}} (\%)$	$X_{\text{H}_2\text{O}_2} (\%)$	$\sum \text{TOC}_{\text{REF}} (\text{mg L}^{-1})$	$\text{Fe}_{\text{leach}} (\text{mg L}^{-1})$	$\text{Fe}_{\text{leach}} (\%)$
Conditions 1	100/500	500	81	96	4.7	2.2	10
Conditions 2	1000/5000	5000	85	100	109.8	32.5	16
Conditions 3	1000/5000	1000	25	50	59.2	15.2	37

initial Fe weight in the catalyst, come also given. To increase ten times all the initial variables in CWPO (condition 2 vs. condition 1) a slightly increase in TOC and H₂O₂ conversions at 240 min can be seen in Table 7 to compare with the first studied conditions. The same intermediates, mainly aromatic and low weight organic acids were detected. The fact that $\sum \text{TOC}_{\text{REF}}$ in conditions 2 (109.8 mg L⁻¹) was more than ten times the value obtained in conditions 1 (4.7 mg L⁻¹) can be indicative of a higher mineralization degree. To try to know the catalyst concentration performance during phenol oxidation process, a third experiment with lower catalyst amount (conditions 3) was also analyzed. From these results a very lower TOC and H₂O₂ conversions (see Table 7) were arisen after 4 h, as it can be expected, given that in this case catalyst concentration was only increased two times respect to the first conditions whereas starting phenol and H₂O₂ concentration was enhanced ten times.

The efficiency of H₂O₂ on phenol oxidation is given in Fig. 7 for the three studied conditions with FeCM-1 catalyst. First of all a very efficient H₂O₂ decomposition to produce hydroxyl radicals capable to oxidize organic matter was arisen when 500 and 5000 mg L⁻¹ of catalyst were used. Higher H₂O₂ efficiency to phenol oxidation was obtained in intermediate times with conditions 2. However 1000 mg L⁻¹ of catalysts in conditions 3 were not enough to get adequate phenol and H₂O₂ conversions, being necessary longer reaction time to get total phenol conversions with significant TOC removal.

3.3. Fe leaching from the catalysts

Higher oxalic acid concentrations gave always rise to higher Fe leaching as can be seen from Fig. 8, thus confirming the detrimental effect of that oxidation product which besides is refractory to CWPO as indicated before.

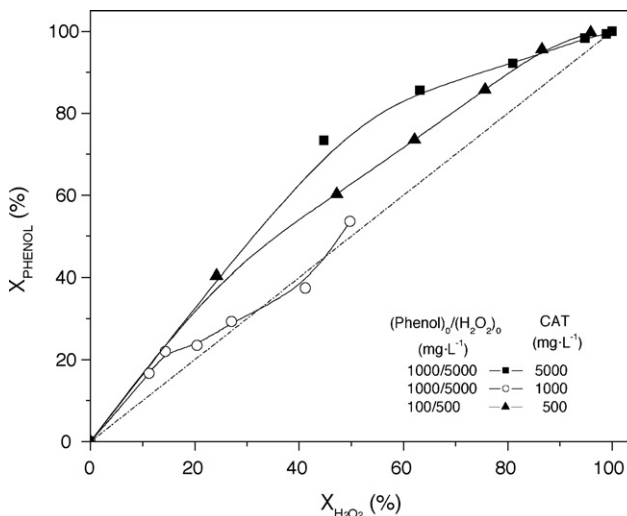


Fig. 7. Evolution of phenol vs. H₂O₂ conversion with FeCM-1 catalyst for the studied operating conditions.

Some experiments were carried out to learn on the stability of the Fe active phase on the catalysts in the presence of oxalic acid. Fig. 9 shows the obtained results. The experiments were performed in batch at the conditions described in the experimental section, using a 25 mg L⁻¹ oxalic acid solution which is above the highest value found in the CWPO experiments after 4 h reaction time (see Fig. 6).

As can be seen a very fast leaching of Fe takes place in the early stages of contact and after about 30–40 min further leaching becomes almost negligible. Iron nitrate leads to more stable anchorage of iron than iron pentacarbonyl except in the case of the CN support where nearly similar Fe leaching is observed. The activated carbon leading to a more stable fixation of Fe is CC in spite of the fact that as discussed before iron is mainly distributed on the external surface. The higher amounts of oxygen groups of acidic character may be one reason for that. In fact, the highest Fe leaching was found for the CM-supported catalyst prepared from iron pentacarbonyl (FeCM-2) which is also the one with a lower amount of acidic or CO₂-evolving groups (see Table 4). The percentage of Fe leached from that catalyst reaches close to 60% after 4 h of contact with the oxalic acid solution.

Finally, respect to the influence of phenol and catalyst concentrations on FeCM-1 catalyst stability, the iron lixiviates to the reaction medium increased to enhance phenol concentration since also oxalic acid concentration increased in the reaction medium (see Table 7). When the operating conditions increased ten times for all the studied variables, a slightly higher percentage of iron leached was detected after 4 h (16%) to compare to the first conditions (10%). However, when the effect of catalyst concentration was studied to compare conditions 2 and 3, lower catalyst concentration led to lower amount of iron lixiviates at 4 h since lower concentration of oxalic acid was reached in spite of the total losses of Fe was around 37% as a consequence of the lower catalyst concentration.

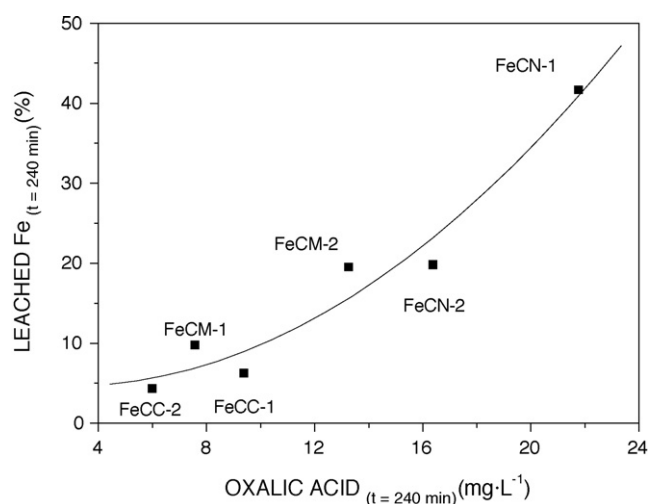


Fig. 8. Influence of oxalic acid concentration on Fe leaching from the catalysts during CWPO of phenol.

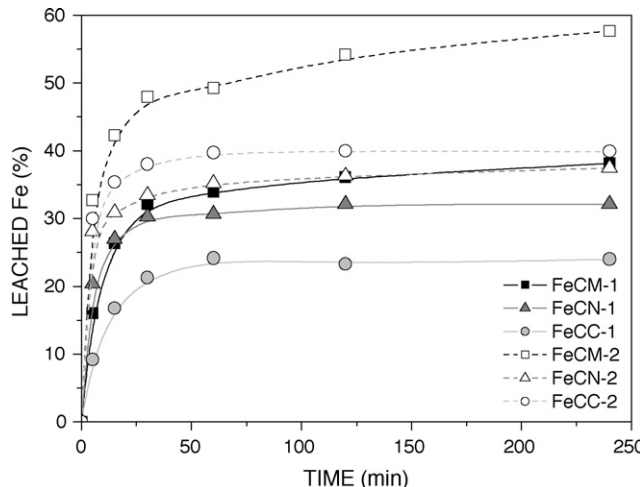


Fig. 9. Fe leaching from the catalysts with 25 mg L⁻¹ oxalic acid solution.

4. Conclusions

The results obtained in CWPO of phenol with several Fe catalysts prepared using different activated carbons as supports reveal the difficulty of predicting the oxidation activity of this type of catalysts since a number of crossed effects need to be considered. These effects refer to the porous structure and the composition of the carbon surface which affect to the Fe distribution onto the catalyst particles. The catalyst with an external or egg-shell type distribution of Fe showed the poorest oxidation activity since it promotes a faster decomposition of H₂O₂ mainly to non-reactive O₂. Although homogeneous distribution of Fe was obtained using iron pentacarbonyl as precursor and a suitable activity was found with their catalysts, lower stability was always addressed compared with the iron nitrate catalysts. The catalysts showing a better activity led to complete phenol conversion and almost 80% mineralization in less than 2 h. Complete disappearance of highly toxic aromatic intermediates was reached. The remaining oxidation by-products were only short-chain organic acids, being the most important one oxalic acid because provokes Fe leaching from the catalysts.

Acknowledgements

The authors wish to thank Prof. J.L.G. Fierro for his help in the AC and Fe/AC characterization studies by XPS. This work has been supported by the Spanish Plan Nacional de I+D+i through the

projects CTM2007-60577/TECNO, CTQ2007-61748/PPQ and CTQ2005-02284/PPQ. Ana Rey thanks to the Ministerio de Educación y Ciencia (MEC) for a FPU Grant.

References

- [1] S.T. Kolaczkowski, P. Plucinski, F.J. Beltrán, F.J. Rivas, D.B. McLurgh, *Chem. Eng. J.* 73 (1999) 143.
- [2] Y.I. Matatov-Meytal, M. Sheintuch, *Ind. Eng. Chem. Res.* 37 (1998) 309.
- [3] K. Pirkanniemi, M. Sillanpää, *Chemosphere* 48 (2002) 1047.
- [4] P.R. Gorate, A.B. Pandit, *Adv. Environ. Res.* 8 (2004) 501.
- [5] F. Luck, *Catal. Today* 53 (1999) 81.
- [6] A.J. Lecloux, *Catal. Today* 53 (1999) 23.
- [7] R. Andreozzi, V. Caprio, A. Insola, R. Martota, *Catal. Today* 53 (1999) 51.
- [8] W.H. Graze, J.W. Kang, D.H. Chapin, *Ozone Sci. Eng.* 9 (1987) 335.
- [9] S. Perathoner, G. Centi, *Top. Catal.* 33 (2005) 207.
- [10] J. Hoigné, H. Bader, *Water Res.* 17 (1983) 185.
- [11] V.S. Mishra, V.V. Mahajan, J.B. Joshi, *Ind. Eng. Chem. Res.* 34 (1995) 2.
- [12] S.T. Hussain, A. Sayari, F. Larachi, *J. Catal.* 201 (2001) 153.
- [13] A. Pintar, M. Besson, P. Gallezot, *Appl. Catal. B Environ.* 31 (2001) 275.
- [14] V. Tukac, J. Vokál, J. Hanika, *J. Chem. Technol. Biotechnol.* 76 (2001) 506.
- [15] A. Pigamo, M. Besson, B. Blanc, P. Gallezot, A. Blakburn, O. Kozynchenko, S. Tennison, E. Crezze, F. Kapteijn, *Carbon* 40 (2002) 1267.
- [16] A. Quintanilla, J.A. Casas, J.J. Rodríguez, *Appl. Catal. B Environ.* 76 (2007) 135.
- [17] F. Stüber, J. Font, A. Fortuny, C. Bengoa, A. Eftaxias, A. Fabregat, *Top. Catal.* 33 (2005) 3.
- [18] A. Quintanilla, N. Menéndez, J. Tornero, J.A. Casas, J.J. Rodríguez, *Appl. Catal. B Environ.* 81 (2008) 105.
- [19] E. González Serrano, T. Cordero, J. Rodríguez Mirasol, J.J. Rodríguez, *Ind. Eng. Chem.* 36 (1997) 4832.
- [20] J.L. Figueiredo, M.F.R. Pereira, M.M.A. Freitas, J.J.M. Orfão, *Carbon* 37 (1999) 1379.
- [21] C. Moreno Castilla, M.V. López Ramón, F. Carrasco Marín, *Carbon* 38 (2000) 1995.
- [22] J.M. Solar, C.A. Leon y Leon, K. Óseo-Asare, L.R. Radovic, *Carbon* 28 (1990) 369.
- [23] C.A. Leon y Leon, L.R. Radovic, in: P.A. Thrower (Ed.), *Chemistry and Physics of Carbon*, Marcel Dekker, New York, 1994, p. 213.
- [24] F. Lücking, H. Köser, M. Jank, A. Ritter, *Water Res.* 32 (1998) 2607.
- [25] J.A. Zazo, J.A. Casas, A.F. Mohedano, J.J. Rodríguez, *Appl. Catal. B Environ.* 65 (2006) 261.
- [26] J.H. Ramírez, F.J. Maldonado-Hodar, A.F. Pérez-Cadenas, C. Moreno-Castilla, C.A. Costa, L.M. Madeira, *Appl. Catal. B Environ.* 75 (2007) 312.
- [27] S.G. Huling, R.G. Arnold, R.A. Sierka, P.K.D.D. Fine, *J. Environ. Eng. ASCE* 126 (2000) 565.
- [28] A. Quintanilla, A.F. Fraile, J.A. Casas, J.J. Rodríguez, *J. Hazard. Mater.* 146 (2007) 582.
- [29] G.M. Eisenberg, *Ind. Eng. Chem. Anal.* 15 (1943) 327.
- [30] E.B. Sandell, *Colorimetric Determination of Traces of Metals*, Interscience Pubs., New York, 1959.
- [31] A. Rey, M. Faraldo, A. Bahamonde, J.A. Casas, J.A. Zazo, J.J. Rodríguez, *Ind. Eng. Chem. Res.* (2008), in press.
- [32] J.F. Moulder, W.F. Stickle, P.E. Sobol, K.D. Bomben, *Handbook of X-ray Photoelectron Spectroscopy: A Reference Book of Standard Spectra for Identification and Interpretation of XPS Data* (Hardcover), Physical Electronics, Reissue ed., 1995.
- [33] C.H. Tessmer, R.D. Vidic, L.J. Uranowski, *Environ. Sci. Technol.* 31 (1997) 1872.
- [34] C.C. Leng, N.G. Pinto, *Carbon* 35 (1997) 1375.
- [35] M.W. Jung, K.H. Ahn, Y. Lee, K.P. Kim, J.S. Rhee, J.T. Park, K.J. Paeng, *Microchim. J.* 70 (2001) 123.
- [36] L.B. Khalil, B.S. Gergis, A.M. Tawfik, *J. Chem. Technol. Biotechnol.* 76 (2001) 1132.
- [37] L. Oliveira, C. Silva, M. Yoshida, R. Lago, *Carbon* 42 (2004) 2279.
- [38] A.F. Fraile, A. Rey, A. Bahamonde, J.A. Zazo, A.F. Mohedano, J.A. Casas, J.J. Rodríguez, *Book Abstr. SECAT* (2007) 75–76.
- [39] F.J. Beltrán, F.J. Rivas, R. Montero-de-Espinosa, *Water Res.* 39 (2005) 3553.